Structural Effects of Hypermodified Nucleosides in the *Escherichia coli* and Human $tRNA^{Lys}$ Anticodon Loop: The Effect of Nucleosides s^2U, mcm^5U, mcm^5s^2U, mnm^5s^2U, t^6A, and ms^2t^6A†

Philippe C. Durant, Ashok C. Bajji, Mallikarjun Sundaram, Raju K. Kumar, and Darrell R. Davis*

Department of Medicinal Chemistry, University of Utah, Salt Lake City, Utah 84112

Received February 23, 2005; Revised Manuscript Received April 8, 2005

ABSTRACT: Previous nuclear magnetic resonance (NMR) studies of unmodified and ψ39-modified $tRNA^{Lys}$ anticodon stem loops (ASLs) show that significant structural rearrangements must occur to attain a canonical anticodon loop conformation. The *Escherichia coli* $tRNA^{Lys}$ modifications mnm^5s^2U34 and t^6A37 have indeed been shown to remodel the anticodon loop, although significant dynamic flexibility remains within the weakly stacked U35 and U36 anticodon residues. The present study examines the individual effects of mnm^5s^2U34, s^2U34, t^6A37, and Mg^{2+} on $tRNA^{Lys}$ ASLs to decipher how the *E. coli* modifications accomplish the noncanonical to canonical structural transition. We also investigated the effects of the corresponding human $tRNA^{Lys,3}$ versions of the *E. coli* modifications, using NMR to analyze tRNA ASLs containing the nucleosides mcm^5U34, mcm^5s^2U34, and ms^2t^6A37. The human wobble modification has a less dramatic loop remodeling effect, presumably because of the absence of a positive charge on the mcm^5 side chain. Nonspecific magnesium effects appear to play an important role in promoting anticodon stacking. Paradoxically, both t^6A37 and ms^2t^6A37 actually decrease anticodon stacking compared to A37 by promoting U36 bulging. Rather than stack with U36, the t^6A37 nucleotide in the free tRNAs is prepositioned to form a cross-strand stack with the first codon nucleotide as seen in the recent crystal structures of $tRNA^{Lys}$ ASLs bound to the 30S ribosomal subunit. Wobble modifications, t^6A37, and magnesium each make unique contributions toward promoting canonical tRNA structure in the fundamentally dynamic $tRNA^{Lys}_{UUU}$ anticodon.

The *Escherichia coli* $tRNA^{Lys}$ and human $tRNA^{Lys,3}$ anticodon loops have closely related hypermodified nucleosides, and their primary loop sequences are identical (*1*). The identical loop sequences for these two tRNAs allowed us to use the 17-nucleotide human $tRNA^{Lys,3}$ anticodon stem loop (ASL)[1] sequence as a common structural context within which to study the structural effects of both the *E. coli* and human modifications (Figure 1). The most interesting questions regarding these $tRNA^{Lys}$ molecules pertain to the function of the hypermodified nucleosides at the wobble position (mcm^5s^2U34 in $tRNA^{Lys,3}$ and mnm^5s^2U34 in *E. coli* $tRNA^{Lys}$) and at the position directly 3′ of the anticodon (ms^2t^6A37 in $tRNA^{Lys,3}$ and t^6A37 in *E. coli* $tRNA^{Lys}$). It has been widely appreciated that modifications in the anticodon domain affect function, and nucleoside modification has been shown to affect ribosome binding (*2*−*4*), missense error rates (*5*), frameshifting frequency (*6*), speed of translation (*7*), and initiation of HIV-1 reverse transcription (*8*, *9*).

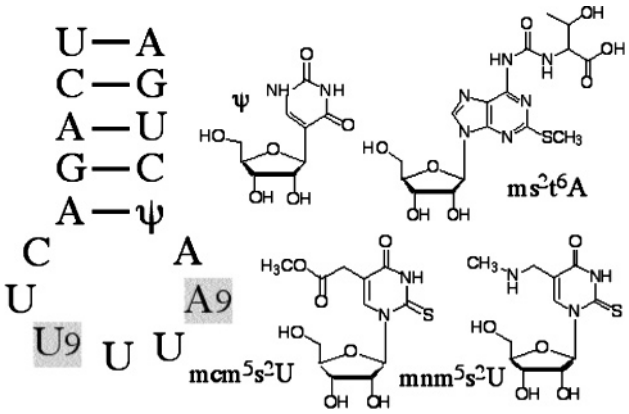

FIGURE 1: ASL secondary structure for human $tRNA^{Lys,3}$ and the modified nucleosides found in human $tRNA^{Lys,3}$ and *E. coli* $tRNA^{Lys}$. Nucleosides U9 (mcm^5s^2U), A9 (ms^2t^6A), and ψ are found in the human tRNA, and mnm^5s^2U, t^6A, and ψ are the corresponding modifications in the single *E. coli* lysine tRNA.

The earlier NMR structures of completely unmodified and ψ39 singly modified human $tRNA^{Lys,3}_{(UUU)}$ ASLs highlighted significant deviations from canonical anticodon loop structure and explained the requirement for modification in the anticodon loop of native lysine tRNAs (*10*). A later NMR structure of the same stem loop with the *E. coli* modifications (mnm^5s^2U34 and t^6A37) showed that hypermodification induces formation of a nearly canonical tRNA anticodon loop; however, the loop uridine riboses still interconvert

† This work was supported by NIH Grant GM55508 to D.R.D., Grants RR06262 and RR13030 for NMR instruments, and Grant CA42014 for RNA synthesis and mass spectrometry.

* To whom correspondence should be addressed. E-mail: davis@alanine.pharm.utah.edu. Telephone: 801-581-7006. Fax: 801-585-9119.

[1] Abbreviations: ASL, anticodon stem loop; NOE, nuclear Overhauser effect; ψ, pseudouridine; mnm^5s^2U, 5-methylaminomethyl,2-thiouridine; mcm^5s^2U, 5-methylcarboxymethyl,2-thiouridine; mcm^5U, 5-methylcarboxymethyl-uridine; s^2U, 2-thiouridine; t^6A, *N*-[(9-β-D-ribofuranosyl-9*H*-purin-6-yl)carbamoyl])-L-threonine; ms^2t^6A, 2-thiomethyl,*N*-[(9-β-D-ribofuranosyl-9*H*-purin-6-yl)carbamoyl])-L-threonine.

10.1021/bi050343f CCC: $30.25
Published on Web 05/11/2005

between the 2′-endo and 3′-endo conformations because of the fundamentally weak uridine stacking (*11*). The X-ray crystal structure of human tRNA^{Lys,3} demonstrated that when the anticodon residues are base-paired the ribose conformation becomes 100% 3′-endo within the context of an A-form RNA duplex (*12*). The *E. coli* tRNA^{Lys} NMR structure showed that modified nucleosides remodeled the noncanonical loop of the ψ39 singly modified ASL, but it did not fully explain how this was accomplished. Several specific questions remained with respect to the loop conformational effects of the *E. coli* modifications and the related human tRNA^{Lys,3} modifications. Here, we report on the specific effects of the s^2 and x^5 modifications that enable mnm^{5}s^{2}U34 and mcm^{5}s^{2}U34 to promote U-turn formation. We also report on the role that (ms^2)t^{6}A37 plays in loop remodeling. Thus, our NMR studies help clarify the individual effects of s^{2}U34, mnm^{5}s^{2}U34, mcm^{5}U34, mcm^{5}s^{2}U34, ms^{2}t^{6}A37, and t^{6}A37 in the context of the tRNA^{Lys,3}-ψ39 ASL.

MATERIALS AND MATERIALS

RNA Synthesis and NMR Sample Preparation. The 17-mer ASLs were synthesized on an Applied Biosystems 394 oligonucleotide synthesizer on a 1 μmol scale. The tRNA^{Lys,3}-ψ39 and tRNA^{Lys,3}-s^{2}U34, ψ39 ASLs were synthesized, deprotected, and purified as described previously (*10*), with the exception that the normal I_2/H_2O oxidation steps were replaced with a 10% tBuOOH solution for oxidation steps in the presence of s^{2}U34 (*11*, *13*). The tRNA^{Lys,3}-mnm^{5}s^{2}U34, ψ39, tRNA^{Lys,3}-t^{6}A37, ψ39, and the native *E. coli* tRNA^{Lys} ASLs were synthesized, deprotected, and purified as described previously (*11*). The ASLs containing the human modifications were also prepared as reported earlier by our laboratory (*14*−*16*).

Careful comparison of different modified ASLs required that each NMR sample be prepared in a rigorously defined fashion. HPLC-purified RNA was dialyzed successively against 5 mM EDTA/50 mM NaCl, 0.1 mM EDTA/50 mM NaCl, 500 mM NaCl/500 mM KCl, 250 mM NaCl/250 mM KCl, and finally deionized water (3×) before lyophilization. NMR buffer was made starting with a 10× solution that results in the final buffer containing 10 mM phosphate buffer at pH 7.5, 50 mM NaCl, 50 mM KCl, and 0.1 mM EDTA. For each sample, 25 μL of 10× NMR buffer was lyophilized and then dissolved in 99.996% D_2O before being combined with the lyophilized RNA sample. The pH of the 250 μL NMR sample was then adjusted to pH ~7.5 before heat annealing at 85 °C followed by rapid cooling in ice. A 0.5 mM $MgCl_2$ solution in 99.9% D_2O was used to bring the Mg^{2+} concentration to 15 mM. The pH was checked and readjusted to pH 7.5 if needed after addition of magnesium. NMR sample concentrations ranged from 0.75 to 2 mM RNA.

NMR Data Acquisition and Analysis. NMR data were collected using Varian Unity 500 MHz and Varian Inova 600 MHz spectrometers fitted with Nalorac probes. All 2D NMR experiments were collected as hypercomplex data sets using TPPI-states phase cycling and processed with Varian VNMR software. Most assignments were obtained from standard 400 ms 2D NOESY (*17*) experiments at 30 °C, but the nonstereospecific assignment of the H5′/H5″ protons was made using 2D two-quantum COSY (*18*) and 2D DQCOSY (*19*) experiments. By convention, the downfield H5′/H5″ resonance is labeled as the H5″ proton. Additional experiments include 1D ^{1}H and ^{31}P spectra and lower mixing time NOESY experiments for some of the ASLs. A 60 ms CBD-NOESY spectrum that minimizes spin diffusion was obtained for the tRNA^{Lys,3}-ms^{2}t^{6}A37, ψ39 ASL for comparison with a standard 60 ms NOESY spectrum (*20*). Imino proton spectra with a spectral width of 11 000 Hz were recorded using the 1−1 solvent suppression scheme at several temperatures (*21*). The 1D ^{31}P spectra were collected using proton decoupling, and proton-detected ^{1}H-^{31}P heteronuclear COSY (*22*) spectra were collected to assign the phosphates. The ^{1}H and ^{31}P spectra were externally referenced to TSP and TMP, respectively.

Criteria Used to Compare Modified ASLs. Our recent NMR structure of the *E. coli* tRNA^{Lys} anticodon loop (i.e., the tRNA^{Lys,3}-mnm^{5}s^{2}U34, t^{6}A37, ψ39 ASL) showed that t^{6}A37 promotes formation of the canonical U33−35p36 interaction and mnm^{5}s^{2}U34 promotes U-turn formation and increases anticodon stacking (*11*). The wobble modifications mnm^{5}s^{2}U and mcm^{5}s^{2}U belong to the x^{5}s^{2}U class of modified nucleosides and each modification (x^5 and s^2) is predicted to affect the loop structure in specific ways that can be monitored by NMR. On the basis of our previous NMR studies (*11*), the x^5 moiety is predicted to alter the dihedral angle of the U-turn phosphate so that the loop attains a more canonical U-turn conformation. The canonical conformation for the 33p34 phosphate is one where the α dihedral angle is trans (*23*), and this is conveniently monitored by ^{31}P NMR because a downfield shift is seen for the phosphate in a U-turn structure (*24*, *25*). The thio moiety in s^{2}U34 is predicted to increase the percentage of 3′-endo ribose conformation (*26*, *27*), increase base stacking within the anticodon triplet (*28*, *29*), and stabilize base pairing with adenosine (*29*−*31*). The extent of base stacking is coupled to the ribose conformation, and the ribose conformation is determined by measuring H1′−H2′ coupling constants, which are then converted to estimates of the percentage of 3′-endo ribose conformation (*32*). In summary, our evaluation of the effects of nucleoside modification on loop structure is mainly through monitoring ^{1}H and ^{31}P chemical-shift changes, ribose conformation changes, and selected NOE changes relative to the reference molecule (tRNA^{Lys,3}-ψ39).

Loop Modeling. Because of the inherent flexibility of these ASLs and the observation that there are few modification-dependent NOEs that unambiguously define a single stable structure, structures were not generated for the purpose of defining modification-dependent root-mean-square deviations or for Protein Data Bank submission. However, structural models were generated for some ASLs for the purpose of testing how well the data fit a particular structural hypothesis. The models were generated using previously determined distance restraints to define the five base pairs of the stem and residues C32 and A38 of the loop (*10*). The region of the loop most affected by modification (U33−A37) was modeled using distance restraints determined from 400 ms 2D NOESY data in D_2O. In some cases, shorter mixing time NOESY spectra (60−200 ms) were also used if spin diffusion issues arose. NOE volumes were converted to distances by scaling to the H5−H6 cross-peaks of uridine and cytidine, and measured distances typically included upper and lower bounds of ±0.5 Å. Structure models were generated using

Table 1: Percentage of 3′-Endo Ribose Conformation and Chemical-Shift Change for the Turning Phosphate (33p34) [15 mM $MgCl_2$ Data Shown in Parentheses]

	U33	U*34	U35	U36	A*37	33p34[a]
$tRNA^{Lys,3}$-ψ39 at pH 5.4	38	22	9	19	64	
$tRNA^{Lys,3}$-ψ39 at pH 7.5	55 (58)	25 (29)	15 (21)	28 (44)	76 (>76)	
$tRNA^{Lys,3}$-mcm^5U34, ψ39	60 (57)	25 (27)	15 (17)	29 (45)	73 (>73)	0.09 (0.07)
$tRNA^{Lys,3}$-s^2U34, ψ39	60	42	15	28	72	0.03
$tRNA^{Lys,3}$-mcm^5s^2U34, ψ39	64 (59)	55 (>55)	19 (42)	31 (31)	76 (>76)	0.35 (0.33)
$tRNA^{Lys,3}$-mnm^5s^2U34, ψ39	67 (86)	60 (>60)	32 (51)	39 (58)	79 (>79)	0.48 (0.83)
$tRNA^{Lys,3}$-t^6A37, ψ39	38 (38)	21 (24)	13 (12)	19 (27)	61 (>61)	−0.11
$tRNA^{Lys,3}$-ms^2t^6A37, ψ39	35 (34)	21 (21)	10 (12)	19 (21)	73 (>73)	−0.13 (−0.26)
$tRNA^{Lys,3}$-mnm^5s^2U34, t^6A37, ψ39	57 (58)	66 (71)	24 (55)	24 (32)	66 (>66)	0.34

[a] A positive chemical-shift change indicates a downfield shift relative to $tRNA^{Lys,3}$-ψ39.

the Discover module of the Insight/Discover program (MSI) and the AMBER force field. Molecular dynamics protocols similar to those described previously were used (*10*, *11*).

RESULTS AND DISCUSSION

Revised Model for the $tRNA^{Lys,3}$-ψ39 ASL. The previously published NMR structures of the unmodified $tRNA^{Lys,3}_{(UUU)}$ ASL and the singly modified $tRNA^{Lys,3}$-ψ39 ASL showed that ψ39 increases the stability of the closing base pair (A31-ψ39) and slightly increases stacking between A37 and A38 (*10*). We also determined that the hypomodified ASLs were very sensitive to pH changes because of protonation of A38 and formation of a C32-A^+38 base pair. At pH 5.4, the A^+-C base pair stabilizes a U33−A37 base pair, and this results in formation of a UUU triloop rather than a canonical U turn. At pH 7, the usual NMR indicators of a canonical U turn are still missing. The turning phosphate (33p34) is not shifted downfield, the anticodon uridines are predominantly in the 2′-endo ribose conformation (Table 1), the strong inter-residue NOEs expected for an A-form anticodon are not seen, and there is no indication of a stable U33 N3H−35p36 phosphate hydrogen bond in the exchangeable proton spectrum. We concluded that the anticodon triplet acts as a dynamic linker between the relatively well-stacked U33 and A37 residues, but it was still possible that our structures were simply underdetermined because of some chemical-shift overlap and incomplete assignments. We have since been able to assign all protons in the $tRNA^{Lys,3}$-ψ39 ASL (and all other ASLs described here), and analysis of the new data confirms our earlier contention that the pH 7 structure is conformationally heterogeneous. The more complete data set also provided greater insight into the conformations that are present in the loop. Because the modifications are evaluated within the context of the $tRNA^{Lys,3}$-ψ39 ASL, we begin the discussion of our current results by describing our revised model for the pH 7 structure of the $tRNA^{Lys,3}$-ψ39 ASL.

Multiple Models Are Consistent with the NMR Data. Although the NOESY data are not consistent with a single anticodon triplet conformation, we were able to use structure defining NOEs to describe conformers likely present within the loop. Population density values for each conformer are not assigned; however, the ease of pH-induced triloop formation suggests that a trilooplike conformer is significantly populated. The rationale for the presence of a trilooplike conformer is based on key A37 H1′−U35 H4′ and U36 H5′/H5″ NOEs (Figure 2A), showing that the backbone of the 35−36 step is stacked under A37 (Figure 3A). In addition, the NOEs describing U36−A37 stacking suggest a bulge conformation that is consistent with a trilooplike structure (i.e., A37 H8−U36 H4′ and H5′/H5″ NOEs) (Figure 2B and Supplementary Figure S1 in the Supporting Information). The proposed trilooplike conformation is basically a more dynamic version of the pH 5 triloop structure resulting from replacement of the C32-A^+38 and U33−A37 base pairs with bifurcated C32/U33 O2−A37/A38 N6H interactions (Figure 3A). The bifurcated U33−A37 interaction should decrease the strain on the loop compared to a canonical U33−A37 pair and likely explains the small increase in 3′-endo ribose conformation for U33 (38 → 55%) and A37 (64 → 76%) when the pH is raised from 5.4 to 7.5 (Table 1). The bifurcated interaction should also be more dynamic than a canonical base pair, making alternate conformations more accessible. Evidence of alternate conformers is manifested by the weak inter-residue H6−H2′/H3′ NOEs of the 400 ms NOESY spectrum (Figure 2C). These NOEs can arise from either a minor population of a dynamic B-RNA-like U turn or from conformational fluctuation of the weakly stacked bases of the triloop. The weak U34 H6−U33 H2′/H3′ NOEs could be formed by a conformer with U33−U34 stacking but probably just reflect the conformational freedom of U34. In summary, there is predominantly a highly populated trilooplike conformer, with at best only a small population of conformers having anticodon stacking.

Magnesium Alters the Population Density of the Conformers by Promoting U36−A37 Stacking. The most significant effect of adding 15 mM $MgCl_2$ is the increase in U36−A37−A38 stacking, as evidenced by the increase in 3′-endo ribose conformation for U36 (28 → 44%) and A37 (76 → ∼100%) (Table 1). The magnesium-induced ^1H chemical-shift changes (Figure 4A) are also concentrated in this region (including U35), indicating that the population of the triloop conformer of Figure 3A has decreased to accommodate increased U36−A37 stacking. The 0.1 ppm downfield shift for the U35 H4′ proton suggests that the backbone of the 35p36 step is less influenced by proximity to A37, as expected for a decreased population of the triloop conformer. When magnesium is added, the U36 H5′/H5″ protons no longer have degenerate chemical shifts and are each shifted 0.1−0.2 ppm downfield. The increased U36−A37 stacking suggested by the U36 ribose conformation is also evidenced by the strong A37 H8−U36 H2′ NOE, while a weaker A37 H8−U36 H4′ NOE (Supplementary Figure S1 in the Supporting Information) indicates that a noncanonical conformation is still present. The broader U36 H1′ and A37 H8 protons indicate altered dynamics, either because of increased U36−A37 stacking

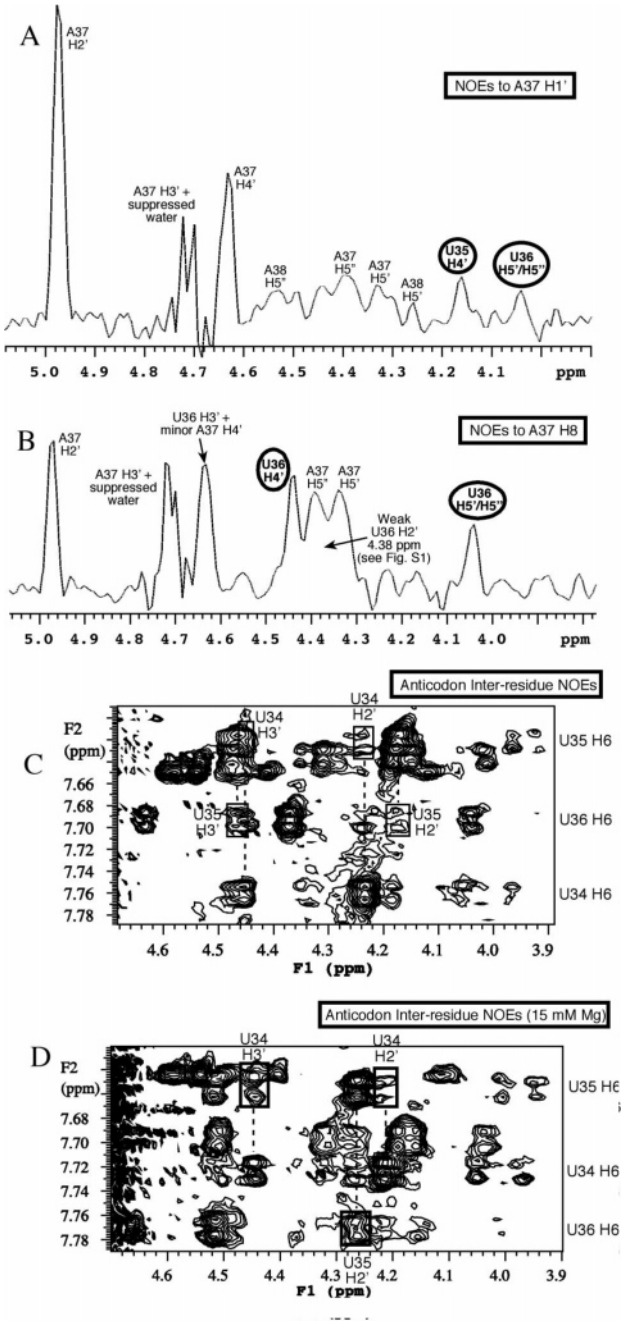

FIGURE 2: tRNA^{Lys,3}-ψ39 400 ms NOESY spectrum collected at pH 7.5 with standard NMR buffer at 30 °C. (A and B) One-dimensional slices of the NOESY spectrum highlighting unusual inter-residue A37−U35/U36 NOEs (circled). (C) Weak inter-residue H6−H2′/H3′ NOEs (boxed) indicative of weak anticodon stacking. (D) Same as in C, but the sample contains 15 mM $MgCl_2$. The U36 H6−U35 H3′ NOE cannot be determined because of overlap with the large U36 H6 to H2′ NOE.

or a change in the interconversion rate between conformers (Supplementary Figure S1 in the Supporting Information).

The A37 H1′−U35 H4′ and the A37 H8−U36 H4′ NOEs show that the Figure 3A triloop is still accessible, if less prevalent. The lack of an imino proton characteristic of a U33 N3H−35p36 interaction, the predominantly 2′-endo riboses, and the weak inter-residue H6−H2′/H3′ NOEs (Figure 2D) argue against a canonical U-turn conformation. Because the low pH and no magnesium data suggest that there is an inherent preference for a closed loop, we propose that the alternate conformation is a closed loop with U36−A37 stacking and a bifurcated U33−A37 interaction (Figure 3B). The minor increase in 3′-endo ribose conformation for U34 (25 → 29%) and U35 (15 → 21%) could easily arise from this alternate triloop whenever the dynamic U33−A37 interaction opens to allow transient formation of a canonical U33−35p36 interaction. The effect of magnesium on the chemical shift, therefore, reflects a general increase in U36−A37 stacking, whether the starting structure is a triloop (ASL with U34) or a U turn with a bulged U36 (ASL with mnm^{5}s^{2}U34, Figure 4).

Implications of the tRNA^{Lys,3}-ψ39 ASL Results. The tRNA^{Lys,3}-ψ39 ASL exhibits several unfavorable structural characteristics that must be corrected by nucleoside modification to form a functional anticodon loop. A canonical anticodon loop conformation is not highly populated in the tRNA^{Lys,3}-ψ39 ASL because of intrinsically low uridine stacking enthalpy, the absence of a hydrogen-bond acceptor/donor at U35 (i.e., no purine N7−U33 2′-OH interaction), and the entropically favored unstacked uridines. The net result is the absence of a thermodynamic driving force to promote a U turn, thereby allowing the relatively weak U33 O2−A37 N6H bifurcated hydrogen bond and van der Waals interactions to dictate the loop conformation by out-competing a canonical U33 N3H−35p36 interaction.

U36 Has a Tendency to Bulge. Recent literature reports suggest that U36 would have a natural tendency to bulge because it is an unpaired uridine and because it is the $n + 3$ uridine of a U turn (*vide infra*). A computational comparison of duplexes containing an unpaired adenosine or uridine shows that adenosine favors a stacked conformation and uridine favors an extra-helical conformation (*33*). Analysis of the bulge trajectories showed that the bulge uridine has a 2′-endo ribose conformation and the 5′ residue can either be 2′-endo or 3′-endo. This would explain why U35 does not adopt a 100% 3′-endo ribose conformation characteristic of an ideal U-turn geometry. In the context of U turns, when the $n + 3$ residue of a U turn is a uridine [as in the GUAA**U**A hexaloop NMR structures (*34*, *35*)], there are conflicting reports on whether the uridine is stacked or bulged. The hexaloop $n + 3$ uridines have the potential to stack between adenosine residues, but stacking apparently depends on salt conditions. Another example is the initiator tRNA$^{Met}_{(CAU)}$ ASL NMR structure, where U36 is only ~24% 3′-endo even though it is between two adenosines and the U turn is well-formed as a result of a purine at position 35 (*36*). Residues C34 and A35 are also dynamic in this tRNA, as shown by the ~50% 3′-endo ribose conformation for these residues, thus highlighting the effects of U36 bulging on residues 34 and 35. Many elongator tRNA^{Met} anticodon loops are modified with a 3′-endo stabilizer to help increase 34−35 stacking (i.e., C_m34 or ac^{4}C34).

Therefore, with or without (ms^2)t^{6}A37, U36 does not contribute interactions that promote a canonical U-turn conformation, and it is the interactions involving U34 and U35 that are the most influential for determining whether anticodon stacking occurs. This again highlights the importance of wobble modification because, unless nucleoside modification is used to enhance 34−35 stacking, closed loop and other noncanonical conformers are highly populated.

Structural Effects of mcm^{5}U34 Modification. Replacing U34 with mcm^{5}U34 has almost no effect on the structure of tRNA^{Lys,3}-ψ39 as evidenced by the lack of ^{1}H chemical-shift

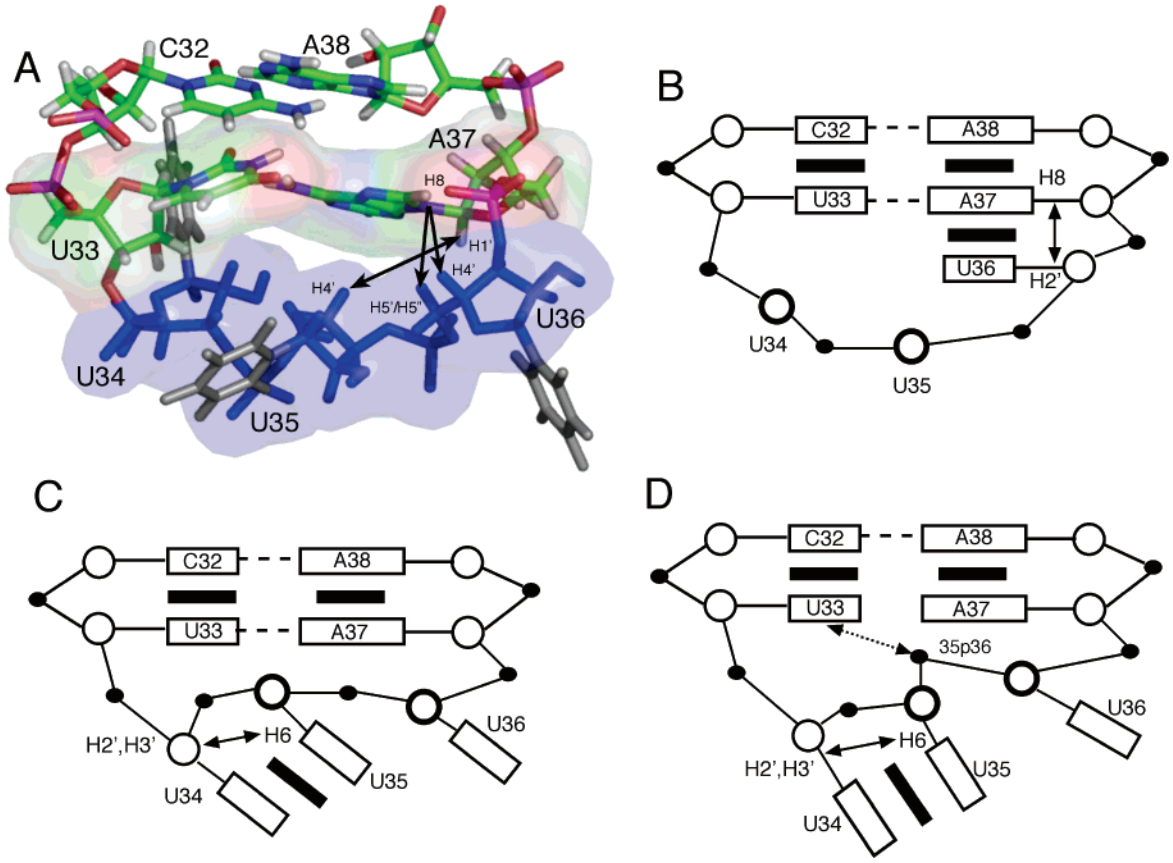

FIGURE 3: (A) pH 7 triloop conformer. Arrows indicate characteristic triloop NOEs. Anticodon riboses are blue, and anticodon bases are gray. (B) Alternate triloop conformer resulting from magnesium-induced U36−A37 stacking; supported by A37 H8−A36 H2′ NOE. (C) Alternate triloop conformer resulting from modification-induced 34−35 stacking and U36 bulging supported by inter-residue NOEs and 3′-endo sugar. (D) Proposed alternate conformer with modification-induced 34−35 stacking, a dynamic U33−35p36 interaction, and a bulged U36, supported by NOEs as in C. Bold circles represent 2′-endo ribose, and thick bars represent stacking interactions. The double arrow in D represents a U33−35p36 phosphate hydrogen bond. The dotted lines represent bifurcated 32/33 O2−37/38 N6H hydrogen bonds.

changes (Figure 4C). The usual NMR indicators of a U turn are still missing, and there is no increase in the percentage of 3′-endo ribose conformation at the wobble position or the other anticodon uridines (Table 1). The NOEs describing anticodon stacking remain very weak (Figure 5A), and the NOEs describing the triloop conformer are unchanged. The NOEs involving the mcm^5 side chain are consistent with all conformers described for the $tRNA^{Lys,3}$-ψ39 ASL. The CH_2−U35 H5 NOE is consistent with the small population of anticodon stacking, and the weak CH_2−U33 H5 NOE is consistent with 33−34 stacking (Figure 6B). The strong CH_2−U33 H4′ NOE (Figure 6B) suggests that a triloop conformation is highly populated. The mcm^5 modification does not appear to inhibit triloop formation because we see an upfield chemical shift for the U35 H4′ proton even at pH 6.9. This proton is significantly shifted upfield in the triloop because of proximity to A37 (Figure 3A). Further evidence that the mcm^5 modification does not stabilize anticodon stacking is the fact that residues 34 and 35 are even more resistant to magnesium-induced stacking effects than in the U34 ASL (Table 1). We conclude that the mcm^5 modification has essentially no effect on the loop conformation and the mcm^5 modification does not inhibit alternate conformations such as a triloop.

Implications for the Function of the mcm^5 Modification. In our discussion above regarding the barriers to remodeling the loop, we stated that U34−U35 stacking is the driving force promoting canonical U-turn formation. At the nucleoside level, the mcm^5 modification has almost no effect on the ribose conformation (U = 12% 3′-endo and mcm^5U = 19% 3′-endo) (*37*); therefore, mcm^5U34 is unable to promote anticodon stacking. In theory, the mcm^5 modification could favor a U turn by forming a hydrogen bond with a nearby functional group, but this does not occur. The methylene protons of the mcm^5 side chain have degenerate chemical shifts and appear as a singlet rather than a doublet (Figure 6A), suggesting that the mcm^5 side chain has complete rotational freedom and does not form a stable hydrogen bond with any nearby functional group. This property of the side chain does not appear to be the result of the noncanonical structure of the $tRNA^{Lys,3}$-mcm^5U34, ψ39 ASL because the same behavior is observed in the more canonical $tRNA^{Lys,3}$-mcm^5s^2U34, ψ39 ASL, the $tRNA^{Lys,3}$-mnm^5s^2U34, ψ39 ASL, and the native *E. coli* $tRNA^{Lys}$ ASL. Thus, any effect of the mcm^5 modification must occur by a steric mechanism, whereby the freely rotating side chain inhibits alternate conformations such as the closed loop conformers. However, steric restriction does not occur in the $tRNA^{Lys,3}$-mcm^5U34, ψ39 ASL because residue 34 is unstacked and the entire nucleoside is free to take almost any conformation. Therefore, the mcm^5 modification most likely influences anticodon structure through a steric mechanism that only functions when 34−35 stacking is induced by the presence of a 2-thio or 2′-*O*-methyl modification.

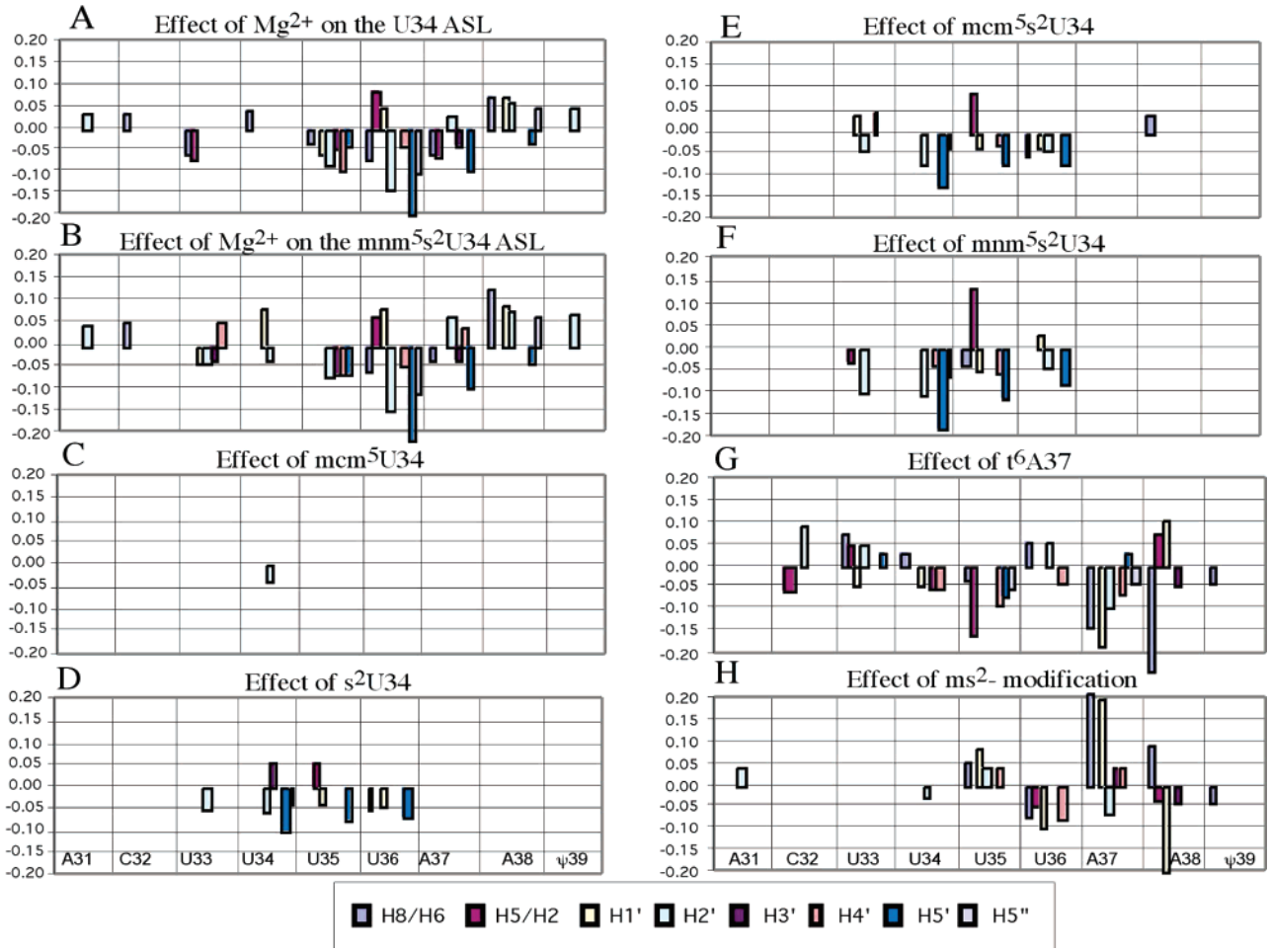

FIGURE 4: Modification- and magnesium-induced ^{1}H chemical-shift changes greater than 0.03 ppm. A negative value indicates that the change in conditions ($MgCl_2$ or modification) shifts the resonance downfield. Effect of magnesium on U34 (A) and mnm^{5}s^{2}U34 (B) ASLs. Effect of modification: (C) mcm^{5}U34, (D) s^{2}U34, (E) mcm^{5}s^{2}U34, (F) mnm^{5}s^{2}U34, (G) t^{6}A37, and (H) ms^2 modification (i.e., comparison of t^{6}A37 and ms^{2}t^{6}A37 ASLs).

s^{2}U34 Shifts the Equilibrium toward 34−35 Stacking. Similar to the U34 and mcm^{5}U34 ASLs, the tRNA^{Lys,3}-s^{2}U34, ψ39 ASL lacks most of the usual NMR indicators of a U turn. The 33p34 phosphate is not shifted downfield, there is no evidence of a U33 N3H−35p36 interaction in the exchangeable proton spectrum, the anticodon triplet is predominantly 2′-endo, and the NOEs describing the triloop conformation of Figure 3A are still observed. However, chemical-shift changes (Figure 4D) show that s^{2}U34 does alter the average structure of the loop, and the stronger inter-residue H6−H2′/H3′ NOEs (Figure 5B) suggest that these chemical-shift changes reflect a shift in equilibrium toward 34−35 stacking. The s^{2}U34 modification promotes 34−35 stacking and inhibits the closed-loop conformers compared to mcm^{5}U34 because it more strongly promotes the 3′-endo ribose conformation. Indeed, compared to U34, s^{2}U34 increases the 3′-endo ribose conformation from 25 to 42% (Table 1). However, this is actually a rather modest effect considering that s^{2}U is 59% 3′-endo at the nucleoside level (*37*) and s^{2}U within an r(Gs^{2}UUUC) single-stranded pentamer is 75% 3′-endo (*29*). In the pentamer, 2-thio modification is also much more effective at increasing the stacking of the following two uridines (to 75% 3′-endo), whereas the ribose conformations of U35 and U36 in the ASL are unchanged by the presence of s^{2}U34. The ribose conformation data implies that the intrinsic ability of s^{2}U34 to promote anticodon stacking is hampered by competing alternate conformations that are still thermodynamically accessible despite the stacking enthalpy contributed by s^{2}U34. Although the 2-thio-promoted increase in 34−35 stacking diminishes the prevalence of the proposed triloop conformation favored by the tRNA^{Lys,3}-ψ39 ASL (Figure 3A), there is little evidence of canonical anticodon stacking, as shown by the very weak U36 H6−U35 H2′ NOE (Figure 5B). The tendency of U36 to bulge likely explains the weak U36 H6−U35 H2′ NOE.

At least two models would be consistent with s^{2}U34−U35 stacking and U36 bulging. In one model, U33 interacts with A37 to form a closed loop (Figure 3C), and in the other model, U33 forms a dynamic canonical interaction with the 35p36 phosphate (Figure 3D). The conclusion from the s^{2}U34 results is that, although the equilibrium is shifted away from the Figure 3A triloop conformation, the loop is still a mixture of conformers and the 2-thio modification alone does not alter the geometry of the 33p34 phosphate.

How Is Such a Dynamic Loop Able to Bind Ribosomes? To explain how s^{2}U34 enhances the ribosome-binding ability of unmodified tRNA^{Lys} (*2*), we suggest that the slight increase in 34−35 stacking modestly contributes to mRNA binding, but the biggest factor is likely the free energy gained by forming a codon−anticodon duplex containing a s^{2}U−A base pair. It has previously been shown that the s^2 modification

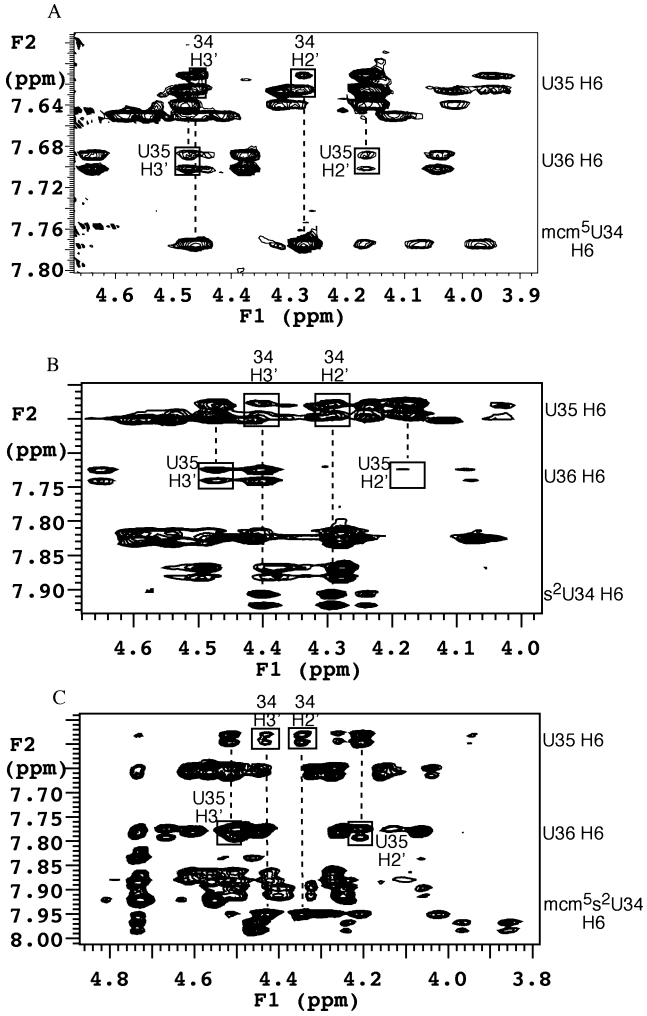

FIGURE 5: NOESY spectra (400 ms) collected at 30 °C. The spectra show inter-residue H6−H2′/H3′ NOEs (boxed) for U35 and U36 when the wobble position is modified to mcm^{5}U34 (A), s^{2}U34 (B), or mcm^{5}s^{2}U34 (C). Samples contain standard NMR buffer with no magnesium.

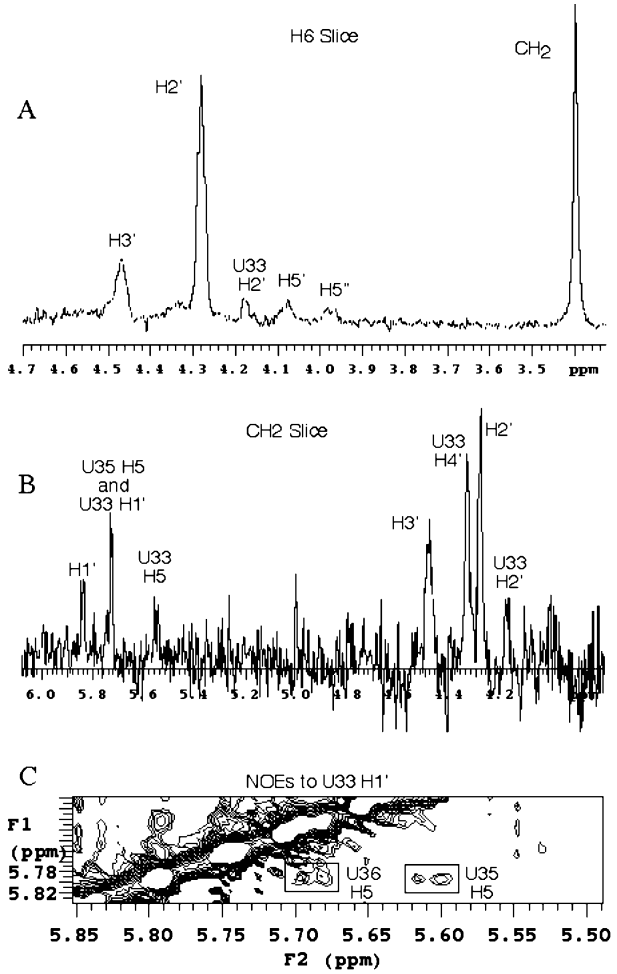

FIGURE 6: (A) Upfield region NOEs for the H6 proton of the mcm^{5}U34 residue. Note the single CH_2 peak indicative of free rotation. (B) NOEs to the CH_2 group of mcm^{5}U34. (C) NOESY data showing magnesium-induced nativelike NOEs for the tRNA^{Lys,3}-mnm^{5}s^{2}U34, ψ39 ASL. All data shown are from 400 ms 2D NOESY spectra in standard NMR buffer. The spectra shown in A and B were obtained in the absence of magnesium.

significantly enhances the stability of RNA duplexes (*29*, *31*). The ability of a more energetically favorable codon−anticodon pairing to compensate for the tRNA^{Lys,3}-s^{2}U34, ψ39 ASL reorganization penalty may also be operable in ribosome-binding experiments with the unmodified human tRNA$^{Lys,1,2}_{(CUU)}$ ASL (*3*). In this case, C34 should not be any more proficient than s^{2}U34 in remodeling the putative trilooplike structure of unmodified tRNA$^{Lys,1,2}_{(CUU)}$, but the formation of a G−C base pair favors induced fit codon binding. The fact that the s^{2}U34 ASL translocates in ribosome-binding experiments reinforces the idea that a stronger codon−anticodon duplex can compensate for a dynamic loop (*38*). The singly modified mnm^{5}U34 and t^{6}A37 ASLs bind programmed ribosomes but do not translocate because of the weak codon−anticodon duplex containing three A−U base pairs.

mcm^{5}s^{2}U34 Increases 34−35 Stacking and Alters 33p34 Geometry. The addition of the mcm^5 modification to s^{2}U34 brings the loop closer to a canonical anticodon conformation. The biggest changes are the 0.3 ppm downfield shift for the 33p34 phosphate resonance, the increase in 3′-endo ribose conformation at the wobble position (42% for s^{2}U34 to 55%, Table 1), and the appearance of a strong U36 H6−U35 H2′ NOE (Figure 5C). The 33p34 ^{31}P chemical-shift change indicates that the average α or ζ dihedral angle has become less A form and shows that the U turn is more defined than with the 2-thio modification alone. The increase in 3′-endo ribose conformation shows that 34−35 stacking is more prevalent but, as with the s^{2}U34 ASL, does not in itself prove that the loop is more canonical because we cannot rule out the presence of a U33−A37 interaction facilitated by U36 bulging (Figure 3C). Fortunately, this point is addressed by a strong U36 H6−U35 H2′ NOE consistent with a conformer with U35−U36 stacking, most likely arising from a continuation of modification-enhanced 34−35 stacking. This single NOE is important because evidence of significant U35−U36 stacking was not observed in the s^{2}U34 ASL, implying that a certain amount of U-turn stability must occur before conformers with U35−U36 stacking are populated to the extent that a strong NOE arises. The small increase in U35 3′-endo ribose conformation (15 → 19%) indicates that there is only a minor increase in the population of conformers with U35−U36 stacking. The relatively strong U36 H6−U35 H2′ NOE can by explained by keeping in mind that ∼90% of the NOE volume can arise from a conformation present only in ∼10% of the time (*39*). Although this modified loop

exhibits more canonical properties, the A37 H1′−U35 H4′ NOE characteristic of a triloop is still present and, on the basis of the minor percentage of 3′-endo ribose population for U35 and U36, U36 still populates a bulge conformation. We interpret the data as indicating that the 2-thio modification of s^{2}U34 increases 34−35 stacking but not to the extent that the U33−35p36 interaction is stabilized or completely favored over the U33−A37 interaction. Adding on the mcm^5 modification further increases 34−35 stacking, alters the dihedral angle of the turning phosphate, and destabilizes the U33−A37 interaction sufficiently that conformers with U35−U36 stacking are transiently populated.

Effect of Magnesium on the tRNA^{Lys,3}-mcm^{5}s^{2}U34, ψ39 ASL. When 15 mM $MgCl_2$ is added to the tRNA^{Lys,3}-mcm^{5}s^{2}U34, ψ39 ASL, 34−35 stacking is strengthened enough to promote a large increase in U35−U36 stacking. The stronger U35−U36 stacking is evidenced by a large increase in the 3′-endo ribose conformation for U35 (19 → 42%), increased chemical-shift dispersion, and nativelike NOEs from the U35 and U36 H5 protons to the U33 H1′ proton (similar to the NOEs shown in Figure 6C for the mnm^{5}s^{2}U34-modified ASL). The results are consistent with a decreased population of the proposed Figure 3C closed-loop conformer, but the relatively high percentage of 2′-endo ribose conformation for U35 and U36 indicate that a canonical U turn is still not highly populated. We favor a model where U36 oscillates between a near-canonical and bulged (Figure 3D) conformation. The addition of magnesium results in a general increase in 34−35−36 stacking, and the loop seems poised at the thermodynamic edge of a canonical U turn.

Implications for the Mechanism of Codon Binding. The results above show that significant anticodon stacking only occurs when the mcm^5 modification is combined with the s^2 modification in the presence of magnesium. The inability of the mcm^{5}side chain to significantly increase codon binding without the added presence of a 3′-endo stabilizing sulfur modification is supported by the modification status of the mammalian tRNA$^{[Ser]Sec}_{(UCA)}$, which must read a UGA stop codon to insert selenocysteine. We predict a dynamic U turn for this tRNA based on sequence similarity with an *E. coli* tRNA$^{Trp}_{(CCA)}$ ASL studied in our laboratory (unpublished results). Two isoforms of tRNA$^{[Ser]Sec}_{(UCA)}$ are present that differ in the extent of modification at the wobble position. When selenium levels are low, the predominant modification is mcm^{5}U34, and when selenium levels increase, the proportion of mcm^{5}U$_m$34 containing tRNA increases (reviewed in ref *40*). The 2′-*O*-methyl modification should have effects similar to the s^2 modification because both promote the 3′-endo conformation. Our studies would predict that the mcm^{5}U-modified tRNA does not read UGA stop codons efficiently, thereby minimizing inappropriate reading of stop codons. It was recently reported that tRNA$^{[Ser]Sec}_{(UCA)}$ without the 2′-*O*-methyl modification is much less efficient at SECIS-directed UGA codon recognition in selenoprotein mRNAs (*41*). These biological observations are consistent with the steric mechanism that we propose for altering the turning phosphate geometry. When the wobble position is not stacked on U35, the wobble base has enough conformational freedom to avoid steric conflict, but when 34−35 stacking is increased by s^2 or 2′-*O*-methyl modification, the turning phosphate α-dihedral angle would become more trans to avoid steric conflict. In other words, the mcm^5 modification has no effect on the structure unless in the context of a stacked mcm^{5}U34−U35 unit.

mnm^{5}s^{2}U34 Shifts the Equilibrium Closer to a Canonical Anticodon Conformation than mcm^{5}s^{2}U34. tRNA ASLs with mnm^{5}s^{2}U have a more stable U turn than mcm^{5}s^{2}U-modified ASLs because of stabilization of the 3′-endo sugar conformation (19 versus 27% 3′-endo at the nucleoside level). The increased 34−35 stacking (mnm^{5}s^{2}U34 is 60% 3′-endo) is propagated to increased U35−U36 stacking (U35 is 32% 3′-endo compared to 19% in the mcm^{5}s^{2}U34 ASL) and to increased U36−A37 stacking (U36 is now 39% 3′-endo). As a result, the 33p34 phosphate geometry is more canonical (shifted 0.5 ppm downfield, Table 1). Thus, the increased ability of mnm^{5}s^{2}U34 to stabilize 34−35 stacking and the increased ability of the mnm^5 modification to stabilize a trans α-dihedral angle for the 33p34 phosphate directly translates into significant 34−35−36−37 stacking. A critical threshold of U-turn stability is attained in the 33−35 region of the loop so that increased 35−36−37 stacking and presumably a stronger U33−35p36 interaction then occurs. However, the loop remains a mixture of conformers, as evidenced by the A37 H1′−U35 H4′ NOE, the lack of an imino proton resonance for U33, and the significant percentage of 2′-endo ribose conformation for the loop uridines.

Magnesium Promotes Anticodon Stacking and Abrogates U36 Bulging. Upon addition of 15 mM magnesium, anticodon stacking increases (Table 1); all uridines are now ∼50% 3′-endo or higher, the 33p34 phosphate is shifted 0.83 ppm downfield compared to the tRNA^{Lys,3}-ψ39 ASL, and the NOE pattern becomes similar to that seen for the native *E. coli* ASL. For example, the U35 and U36 H5 protons now show NOEs to the U33 H1′ proton (Figure 6C). The observed nonspecific magnesium effects appear to be synergistic with the conformational stabilization promoted by the mnm^{5}s^{2}U34 modification, resulting in a higher prevalence of anticodon stacking. Magnesium also appears to reduce the bulging of U36 as evidenced by a stronger A37 H8−U36 H2′ NOE and much weaker A37 H8−U36 H4′ NOE. In fact, anticodon stacking is more canonical in the tRNA^{Lys,3}-mnm^{5}s^{2}U34, ψ39 ASL than the *E. coli* tRNA^{Lys} ASL because t^{6}A37 promotes U36 bulging. It is interesting that the magnesium effects for U36−A37 stacking are much greater in tRNA^{Lys,3}-mnm^{5}s^{2}U34, ψ39 ASL compared to the tRNA^{Lys,3}-mcm^{5}s^{2}U34, ψ39 ASL (58 versus 31% 3′-endo ribose conformation for U36). This appears to be as a direct result of a more rigid conformation from positions U33 to U35 that increases the prevalence of the canonical U33−35p36 interaction. Thus, in the context of the tRNA^{Lys,3}-mnm^{5}s^{2}U34, ψ39 ASL, there is sufficient stacking that nonspecific magnesium effects are able to further promote 36−37 stacking. Nevertheless, the lack of a U33 N3H resonance and the tendency of U36 to bulge (as evidenced by the A37 H8−U36 H4′ NOE) shows that considerable dynamics remain in this region.

Effect of t^{6}A37 on the tRNA^{Lys,3}-ψ39 ASL. Incorporation of t^{6}A37 into an unmodified tRNA^{Lys} ASL enables binding to poly-A programmed ribosomes (*3*, *4*) and allows formation of a stable complex between tRNA^{Lys,3}-ψ39 and the HIV-1 A-rich loop (*15*). Previous hypotheses regarding the function of t^{6}A37 point to the probability that it inhibits base pairing with residues on the 5′ side of the loop, and it was suggested

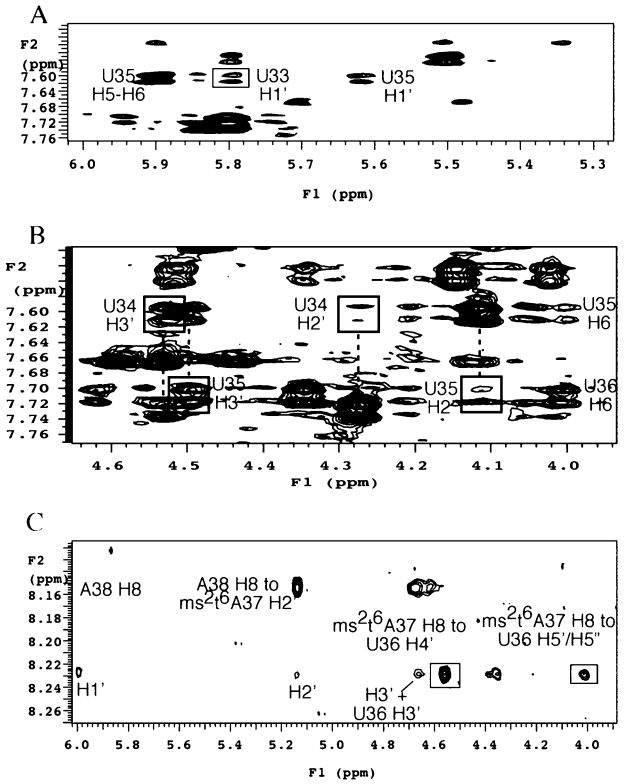

FIGURE 7: (A) Base to H5/H1′ region of a 400 ms 2D NOESY spectrum of the tRNA^{Lys,3}-ms^{2}t^{6}A37, ψ39 ASL showing nativelike U35 H6−U33 H1′ NOE. (B) Base to sugar region of the same spectrum as in A showing inter-residue H6−H2′/H3′ NOEs for anticodon residues U35 and U36. (C) NOESY spectrum (60 ms) showing unusual ms^{2}t^{6}A37 H8−U36 H4′ and H5′/H5″ NOEs indicative of a bulged U36.

that t^{6}A increases base stacking (*42*, *43*). We have previously used imino and ^{31}P spectra of tRNA^{Lys,3}-t^{6}A37, ψ39 to qualitatively determine which properties of the fully modified *E. coli* tRNA^{Lys} ASL were due to mnm^{5}s^{2}U34 and which were due to t^{6}A37 (*11*). The appearance of a weak imino resonance at ~11.4 ppm in t^{6}A37-modified ASLs suggested that t^{6}A37 somehow stabilized the canonical U33 N3H−35p36 phosphate hydrogen bond, and we assumed that this occurred by increased base stacking of the anticodon uridines. It now seems clear that the main reason a U33 imino resonance is not seen for the tRNA^{Lys,3}-ψ39 ASL is because closed-loop conformers compete with formation of the canonical U33−35p36 phosphate interaction. When t^{6}A37 is present, U33 can no longer pair with A37 and this allows U33 to interact with the 35p36 phosphate. The evidence for this specific interaction is that the chemical shift is indicative of an imino−oxygen hydrogen bond and the U35 H6−U33 H1′ NOE places the 35p36 phosphate proximal to U33 (a similar NOE is shown in Figure 7A for the ms^{2}t^{6}A37-modified ASL).

t^{6}A37 Has Unexpected Effects on the Loop Structure. We have gone back and investigated the function of t^{6}A37 in detail and were surprised to find that t^{6}A37 actually decreases base stacking within the anticodon loop. As shown in Table 1, residues 33−36 all have a decreased percentage of 3′-endo conformation when t^{6}A is present and t^{6}A37 itself shows a decrease in 3′-endo conformation from 76 to 61% compared to A37. The narrow line widths and large H1′−H2′ coupling constants for the (ms^2)t^{6}A37-modified ASLs are consistent with a dynamic anticodon loop and provide ideal double-quantum COSY spectra for determination of ribose conformations (see Supplementary Figure S2 in the Supporting Information for a spectrum of the ms^{2}t^{6}A37-modified ASL). Also, U36 appears to bulge relative to position 37 significantly more than in the tRNA^{Lys,3}-ψ39 ASL. The noncanonical 37 H8−U36 H4′ and H5′/H5″ NOEs (similar to the NOE seen for the ms^{2}t^{6}A37-modified ASL in Figure 7C) have a greater volume, and there is a decrease in the U36 3′-endo ribose conformation from 28 to 19%. This behavior is unexpected because inhibiting a closed loop 33−37 interaction should allow stabilization of a U turn with a canonical U33−35p36 interaction. However, the 33−35p36 interaction is dynamic (a U33 imino proton is not observed in the ms^{2}t^{6}A-modified ASL), the uridine stacking is weak, and the lack of a purine at position 35 is problematic. When the U33−35p36 interaction is broken, many conformations are accessible to the anticodon triplet because there is little stacking enthalpy contribution for uridines. When the U33−35p36 interaction is present, U36 tends to bulge because it is the $n + 3$ uridine in a U turn and because t^{6}A37 abrogates 36−37 stacking (discussed below). Residue U34 at the helix terminus should have significant flexibility even with the U33−35p36 interaction. We see highly 2′-endo riboses, suggesting that multiple conformers are present, with the NOE data suggesting that among these conformers are near-canonical conformations giving rise to weak inter-residue H6−H2′/H3′ NOEs and a U35 H6−U33 H1′ NOE (parts A and B of Figure 7). The inter-residue NOEs indicate that canonical A-form 34−35−36 stacking is not significantly populated. Interconversion between conformations is likely quite rapid because degenerate H5′/H5″ chemical shifts are seen for U36 and t^{6}A37, indicating that dihedral angles near the 35p36 and 36p37 phosphates have motion on the chemical-shift time scale. Chemical shifts have changed extensively, indicating that the average position of almost all loop residues is altered (Figure 4G). The lack of magnesium effects on ribose conformation indicates that the anticodon uridines are so weakly stacked that neutralization of the phosphate backbone does not further increase stacking. In summary, t^{6}A37 inhibits the 33−37 interaction, but it does not stabilize a canonical U turn or eliminate alternate conformations.

t^{6}A37 Alters 37−38 Helical Twist. We believe that the key property of t^{6}A37 is the change in helical twist that occurs at position 37 as a result of the side-chain methyl group occupying the same plane of space as A38 (Figure 8A). Our latest results confirm the encroachment of the methyl group into the same plane of space occupied by A38 because we see NOEs from the methyl group to the H1′ and H4′ protons of ψ39. The net result of this region of steric clash is that, compared to A37, t^{6}A37 has increased helical twist with respect to A38. The change in helical twist and inhibition of the closed loop is reflected in the chemical-shift changes seen for positions 37 and 38 on the 3′ side of the loop and positions 32 and 33 on the 5′ side (Figure 4G). The increased anticodon flexibility of the tRNA^{Lys,3}-t^{6}A37, ψ39 ASL compared to the tRNA^{Lys,3}-ψ39 ASL can be explained by the combination of a more open loop that is even less tightly packed than a canonical tRNA and the decreased stacking of U36 with position 37 (note the small overlapping surface area for 36 and 37 in Figure 8A). The

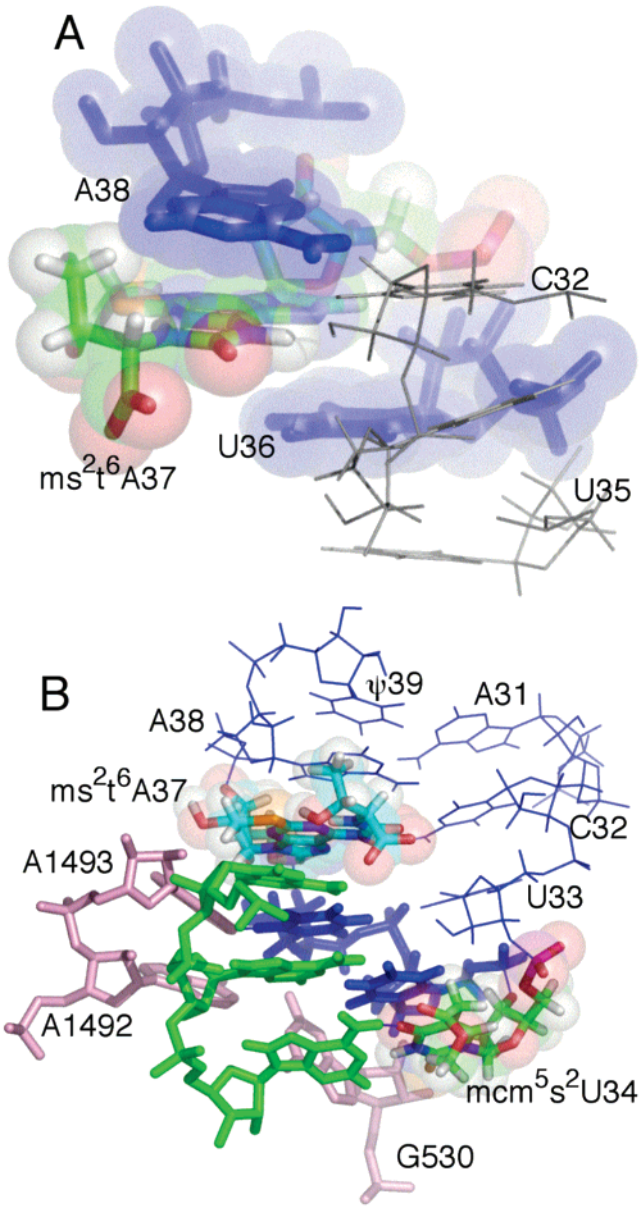

FIGURE 8: (A) Model of the region surrounding ms^{2}t^{6}A37 based on the previously published crystal structure (*12*). The t^{6}A37 side chain and the ms^2 modification were not defined in the crystal structure but are modeled here based on NOE data. Residues 32, 33, and 35 are black wireframe, and U36 and A38 are blue sticks. Note the clash of the ms^{2}t^{6}A methyl with A38 and the lack of overlap of ms^{2}t^{6}A and U36 (B) Same model as in A is docked into the crystal structure of the ribosomal A site (*47*). This model highlights the potential for the t^{6}A37 side chain to hydrogen bond with the first adenosine of the codon and the extensive stacking of ms^{2}t^{6}A37 over this adenosine. The space filling of the mcm^5 side chain highlights the fact that free rotation may be restricted when bound to the ribosome. Ribosomal residues G530, A1492, and A1493 are pink, the mRNA is green, and U35 and 36 are blue sticks.

increased helical twist also weakens 36−37 stacking in the context of the native *E. coli* tRNA^{Lys} ASL. As shown in Table 1, the gain in 36−37 stacking because of the presence of mnm^{5}s^{2}U34 is lost when t^{6}A37 is added to the ASL (U36 drops from 39 to 24% 3′-endo). Thus, the main effect of t^{6}A37 is to alter the helical twist at the 37−38 step, decrease 36−37 stacking, and allow U33 to form a dynamic hydrogen bond with the 35p36 phosphate.

A Proposal for How t^{6}A37 Enhances Ribosome Binding. The t^{6}A "cure" for weak binding seems to be counterintuitive at the loop level because anticodon flexibility is actually increased. However, the net result of the change in helical twist at the 37−38 step is that residue 37 is now prepositioned in a codon-bound conformation where it can stack over the first adenosine of the codon (Figure 8B). This effect of t^{6}A37 is clearly illustrated by the recent crystal structure of the t^{6}A-modified ASL bound to the 30S ribosomal subunit (*44*).

The fact that programmed ribosome and HIV A-rich loop binding is still rather weak for t^{6}A-modified ASLs is consistent with our data showing that t^{6}A37 does not stabilize a rigid, canonical anticodon loop conformation (*3*, *4*, *15*). The weak binding in the *in vitro* assays shows that prepositioning for optimal codon stacking barely compensates for the dynamics of the anticodon loop. A t^{6}A-modified ASL did not translocate in an *in vitro* translocation assay (*38*). A human mitochondrial disease is caused by the lack of a wobble modification (the taurinomethyl group) that significantly reduces translation of the cognate codon (*45*). This tRNA still contains t^{6}A37, showing again that t^{6}A modification alone is not sufficient to compensate for the weak anticodon stacking that results from the lack of wobble modification. Adding 15 mM magnesium does not significantly alter the structure of the t^{6}A-modified ASLs, because the percentage of 3′-endo ribose conformation for the uridines in the t^{6}A37 and ms^{2}t^{6}A37-modified ASLs is essentially unchanged (Table 1).

Effect of ms^{2}t^{6}A37 on the tRNA^{Lys,3}-ψ39 ASL. The human ms^{2}t^{6}A37 modification has essentially the same structural effects on stacking as t^{6}A37, except that ms^{2}t^{6}A37 is slightly more 3′-endo (73 versus 61%). It has been shown at the nucleoside level that the 3′-endo conformation is slightly less favored for t^{6}A compared to adenosine, but the equivalent data for ms^{2}t^{6}A are not available (*46*). NOEs from the CH_3 protons of the threonyl side chain are similar to that seen for t^{6}A37. NOEs from the SCH_3 methyl group are not consistent with a single conformation and indicate that either the thiomethyl group or ms^{2}t^{6}A37 itself has significant conformational freedom. The NH11 imino resonance is involved in a hydrogen bond with the base N1 position but is somewhat weaker than that seen with t^{6}A37 (*11*, *16*), suggesting that the presence of the SCH_3 group may weaken this interaction. The 33−35p36 interaction also appears to be weaker than in the t^{6}A ASL because we do not observe a U33 imino proton in the exchangeable spectrum. The U35 and U36 chemical-shift differences induced by the ms^2 modification are likely due to the weaker 33−35p36 interaction (Figure 4H). We believe that the main function for the ms^2 group is to further increase the strength of the codon−anticodon interaction by stacking over the first adenosine nucleoside of the codon. The ms^2 modification has been shown to significantly enhance binding in ms^{2}i^{6}A-modified tRNAs. As mentioned in the previous section, the t^{6}A side chain likely enhances the effect of the SCH_3 modification by prepositioning residue 37 for stacking on the codon. The interaction of tRNA^{Lys} with the HIV A loop is significantly stabilized for ms^{2}t^{6}A37 compared to t^{6}A37 (350 μM versus 2.4 mM K_D at 1 M NaCl, 4 °C) (*15*). The additional ms^2 modification in human tRNA^{Lys,3} is likely needed to compensate for the more dynamic U turn when the wobble

position is modified with mcm^{5}s^{2}U34 instead of mnm^{5}s^{2}U34. Both the native *E. coli* and human tRNA^{Lys} ASLs have canonical tRNA conformations and bind the HIV A loop with low micromolar K_D values (*11*, *12*, *15*).

CONCLUSIONS

Mechanism for U Turn Stabilization. The comparison of mcm^{5}U34-, s^{2}U34-, and mcm^{5}s^{2}U34-modified tRNA^{Lys,3} ASLs enables us to suggest a steric mechanism for U-turn stabilization by the x^5 side chain of wobble nucleosides. The slight 0.09 ppm downfield shift of the 33p34 phosphate caused by mcm^{5}U34 is consistent with a weak steric effect of the freely rotating mcm^5 side chain on the average position of residue 34 and 33p34 phosphate geometry. The effects are minor because, in the absence of the 2-thio modification, the weak 34−35 stacking allows steric conflict involving the mcm^5 side chain to be avoided without forcing formation of the energetically unfavorable trans α-dihedral angle. The s^2 modification of mcm^{5}s^{2}U34 increases 34−35 stacking, thereby restricting the conformational freedom of the wobble nucleoside. A more trans α-dihedral angle for 33p34 is then required to diminish steric clash involving the mcm^5 or mnm^5 side chains. Thus, mcm^{5}U only affects the 33p34 dihedral angle in a context where there is also good 34−35 stacking (i.e., s^{2}U34 or U$_m$34). Our data hints at the possibility that mcm^{5}U34 prefers to be unstacked relative to U35. Thus, there is a distinct possibility that mcm^{5}U34 in tRNA$^{[Ser]Sec}_{(UCA)}$ is unstacked to avoid steric conflict and the ensuing 2′-O-methylation of mcm^{5}U34 in the presence of selenocysteine acts as a conformational switch that ensures 34−35 stacking for efficient reading of stop codons. The mnm^{5}s^{2}U34-modified ASL displays more U-turn promotion and increased anticodon stacking compared to mcm^{5}s^{2}U34 because the mnm^5 side chain stabilizes the 3′-endo conformation more effectively than mcm^5 and the positively charged amino group may partially neutralize nearby phosphates. The mnm^5 side chain could also stabilize the codon−anticodon duplex by charge neutralization upon duplex formation. The combination of the positively charged side chain and a more structured U turn results in a 7-fold increase in the binding affinity of tRNA^{Lys,3}-mnm^{5}s^{2}U34, ψ39 for the HIV-1 A-rich loop compared to tRNA^{Lys,3}-mcm^{5}s^{2}U34, ψ39 (350 μM versus 2.6 mM). Both mnm^5 and mcm^5 appear to have free rotation; therefore, this may be a common mechanism for U-turn stabilization that is used by other chemically diverse modified wobble nucleosides such as taurinomethyl-modified uridine (*45*) and queosine. Modeling exercises suggest that free rotation is less likely when bound to the ribosomal A site, especially for mcm^{5}s^{2}U34 (Figure 8B). Steric clash in the A site, combined with the structural stabilization afforded by codon binding, may enable formation of a hydrogen bond involving the x^5 modification. The tRNA^{Lys} ASL complex with the 30S subunit supports the notion that the mcm^5 and mnm^5 side chains have a primarily steric function as opposed to making specific structural interactions (*44*).

Function of the ms^2 Modification of ms^{2}t^{6}A37. The t^{6}A37 and ms^{2}t^{6}A37 modifications both decrease anticodon base stacking and inhibit a noncanonical U33−A37 interaction. The ms^2 side chain has little structural effect on the free tRNA^{Lys,3} ASL but is likely needed to compensate for the relatively weak U-turn remodeling properties of mcm^{5}s^{2}U34. According to the tRNA sequence database, the ms^2 modification of t^{6}A37 is rarely used, being found only in mammalian tRNA^{Lys} molecules with mcm^{5}s^{2}U34 and not in tRNA^{Lys} molecules with C34 (*1*). The only known exception is *Bacillus subtilus* tRNA^{Lys}, which contains cmnm^{5}s^{2}U34.

tRNA^{Lys} Anticodon Never Becomes Rigid. The results presented here show how difficult it is to force a UUU anticodon triplet to stack in a completely rigid, canonical conformation. The U36 nucleoside is never 100% 3′-endo, even with high concentrations of magnesium. These results also point to why t^{6}A37 is present in almost all tRNAs with a U36. Inhibition of across-the-loop interactions is not the main reason in our view because many anticodon loop sequences, such as tRNA^{Met}, do not have problems with across-the-loop base pairing. Also, there are many simpler modifications suitable for inhibiting inappropriate base pairing. The general purpose of t^{6}A37 modification appears to be to strengthen codon binding by positioning residue 37 for stacking over the first anticodon−codon base pair. Thus, the positive effect of t^{6}A37 modification (prepositioning of position 37) appears to be balanced out by increased loop flexibility. Modeling of t^{6}A37 in the ribosomal A site shows the potential for additional hydrogen bonds, indicating that the potentially neutral effects of t^{6}A37 modification may be supplemented with hydrogen bonds involving the t^{6}A side chain (Figure 8B). Although the tRNA^{Lys,3} anticodon loop is rather unusual compared to most tRNAs, we believe that the arguments presented here explain the near universal presence of t^{6}A37 in tRNAs that read adenosine in the first codon position. The remarkable conservation of t^{6}A37 throughout biology highlights the importance of a proper geometry for the first codon−anticodon pair when binding to the ribosomal A site.

SUPPORTING INFORMATION AVAILABLE

Two-dimensional NOESY spectra for tRNA^{Lys,3}-ψ39 and two-dimensional DQCOSY spectrum of tRNA^{Lys,3}-ms^{2}t^{6}A37. This material is available free of charge via the Internet at http://www.pubs.acs.org.

REFERENCES

1. Sprinzl, M., Horn, C., Brown, M., Ioudovitch, A., and Steinberg, S. (1998) Compilation of tRNA sequences and sequences of tRNA genes, *Nucleic Acids Res. 26*, 148−153.
2. Ashraf, S., Sochacka, E., Cain, R., Guenther, R., Malkiewicz, A., and Agris, P. (1999) Single atom modification (O−S) of tRNA confers ribosome binding, *RNA 5*, 188−194.
3. Yarian, C., Marszalek, M., Sochacka, E., Malkiewicz, A., Guenther, R., Miskiewicz, A., and Agris, P. F. (2000) Modified nucleoside dependent Watson−Crick and wobble codon binding by tRNA^{Lys}UUU species, *Biochemistry 39*, 13390−13395.
4. Yarian, C., Townsend, H., Czestkowski, W., Sochacka, E., Malkiewicz, A. J., Guenther, R., Miskiewicz, A., and Agris, P. F. (2002) Accurate translation of the genetic code depends on tRNA modified nucleosides, *J. Biol. Chem. 277*, 16391−16395.
5. Hagervall, T. G., Pomerantz, S. C., and McCloskey, J. A. (1998) Reduced misreading of asparagine codons by *Escherichia coli* tRNA^{Lys} with hypomodified derivatives of 5-methylaminomethyl-2-thiouridine in the wobble position, *J. Mol. Biol. 284*, 33−42.
6. Brierley, I., Meredith, M. R., Bloys, A. J., and Hagervall, T. G. (1997) Expression of a coronavirus ribosomal frameshift signal in *Escherichia coli:* Influence of tRNA anticodon modification on frameshifting, *J. Mol. Biol. 270*, 360−373.
7. Kruger, M., Pedersen, S., and Hagervall, T. (1998) The modification of the wobble base of tRNA^{Glu} modulates the translation rate of glutamic acid codons *in vivo*, *J. Mol. Biol. 284*, 621−631.
8. Isel, C., Lanchy, J.-M., Le Grice, S. F. J., Ehresmann, C., Ehresmann, B., and Marquet, R. (1996) Specific initiation and

switch to elongation of human immunodeficiency virus type 1 reverse transcription requires the post-transcriptional modifications of primer tRNA^{Lys,3}, *EMBO J. 15*, 917−924.
9. Isel, C., Marquet, R., Keith, G., Ehresmann, C., and Ehresmann, B. (1993) Modified nucleotides of tRNA^{Lys,3} modulate primer/template loop−loop interaction in the initiation complex of HIV-1 reverse transcription, *J. Biol. Chem. 268*, 25269−25272.
10. Durant, P. C., and Davis, D. R. (1999) Stabilization of the anticodon stem-loop of tRNA^{Lys,3} by an A^{+}-C base-pair and by pseudouridine, *J. Mol. Biol. 285*, 115−131.
11. Sundaram, M., Durant, P. C., and Davis, D. R. (2000) Hypermodified nucleosides in the anticodon of tRNA^{Lys} stabilize a canonical U-turn structure, *Biochemistry 39*, 12575−12584.
12. Benas, P., Bec, G., Keith, G., Marquet, R., Ehresmann, C., Ehresmann, B., and Dumas, P. (2000) The crystal structure of HIV reverse-transcription primer tRNA^{Lys,3} shows a canonical anticodon loop, *RNA 6*, 1347−1355.
13. Kumar, R. K., and Davis, D. R. (1995) Synthesis of oligoribonucleotides containing 2-thiouridine: Incorporation of 2-thiouridine phosphoramidite without base protection, *J. Org. Chem. 60*, 7726−7727.
14. Bajji, A., and Davis, D. R. (2000) Synthesis and biophysical characterization of tRNA^{Lys,3} anticodon stem-loop RNAs containing the mcm^{5}s^{2}U nucleoside, *Org. Lett. 2*, 3865−3868.
15. Bajji, A. C., Sundaram, M., Myszka, D. G., and Davis, D. R. (2002) An RNA complex of the HIV-1 A-loop and tRNA^{Lys,3} is stabilized by nucleoside modifications, *J. Am. Chem. Soc. 124*, 14304−14305.
16. Bajji, A. C., and Davis, D. R. (2002) Synthesis of the tRNA^{Lys,3} anticodon stem-loop domain containing the hypermodified ms^{2}t^{6}A nucleoside, *J. Org. Chem. 67*, 5352−5358.
17. Jeener, J., Meier, B. H., Bachmann, P., and Ernst, R. R. (1979) Investigation of exchange processes by two-dimensional NMR spectroscopy, *J. Chem. Phys. 71*, 4546−4553.
18. Bishop, K. D., Borer, P., and Pelczer, I. (1996) Improved proton assignment for DNA by application of aliasing and dispersive-absorptive phasing to two-quantum COSY spectra, *J. Magn. Reson. 110*, 9−15.
19. Piantini, U., Sorenson, A. W., and Ernst, R. R. (1982) Multiple quantum filters for elucidating NMR coupling networks, *J. Am. Chem. Soc. 104*, 6800−6801.
20. Hoogstraten, C., and Pardi, A. (1998) Improved distance analysis in RNA using network-editing techniques for overcoming errors due to spin diffusion, *J. Biomol. NMR 11*, 85−95.
21. Hore, P. J. (1983) Solvent suppression in Fourier transform nuclear magnetic resonance, *J. Magn. Reson. 55*, 283−300.
22. Sklenar, V., and Bax, A. (1987) Measurement of ^{1}H-^{31}P NMR coupling constants in double-stranded DNA fragments, *J. Am. Chem. Soc. 109*, 7525−7526.
23. Saenger, W. (1984) *Principles of Nucleic Acid Structure*, Springer-Verlag, New York.
24. Jucker, F. M., and Pardi, A. (1995) GNRA tetraloops make a U-turn, *RNA 1*, 219−222.
25. Schweisguth, D. C., and Moore, P. B. (1997) On the conformation of the anticodon loops of initiator and elongator methionine tRNAs, *J. Mol. Biol. 267*, 505−519.
26. Szweykowska-Kulinska, Z., Senger, B., Keith, G., Fasiolo, F., and Grosjean, H. (1994) Intron-dependent formation of pseudouridines in the anticodon of *Saccharomyces cerevisiae* minor tRNA^{Ile}, *EMBO J. 13*, 4636−4644.
27. Yokoyama, S., Yamaizumi, Z., Nishmura, S., and Miyazawa, T. (1979) ^{1}H NMR studies on the conformational characteristics of 2-thiopyrimidine nucleotides found in transfer RNAs, *Nucleic Acids Res. 6*, 2611−2626.
28. Smith, W. S., Sierzputowska-Gracz, H., Sochacka, E., Malkiewicz, A., Agris, P. F. (1992) Chemistry and structure of modified uridine dinucleosides are determined by thiolation, *J. Am. Chem. Soc. 114*, 7989−7997.
29. Kumar, R. K., and Davis, D. R. (1997) Synthesis and studies on the effect of 2-thiouridine and 4-thiouridine on sugar conformation and RNA duplex stability, *Nucleic Acids Res. 25*, 1272−1280.
30. Nair, T. M., Myszka, D. G., and Davis, D. R. (2000) Surface plasmon resonance kinetic studies of the HIV TAR RNA kissing hairpin complex and its stabilization by 2-thiouridine modification, *Nucleic Acids Res. 28*, 1935−1940.
31. Testa, S. M., Disney, M. D., Turner, D. H., and Kierzek, R. (1999) Thermodynamics of RNA−RNA duplexes with 2- or 4-thiouridines: Implications for antisense design and targeting a group I intron, *Biochemistry 38*, 16655−16662.
32. Altona, C. (1982) Conformational analysis of nucleic acids: Determination of backbone geometry of single-helical RNA and DNA in aqueous solution, *J. Royal Neth. Chem. Soc. 101*, 413−433.
33. Zacharias, M., and Sklenar, H. (1999) Conformational analysis of single-base bulges in A-form DNA and RNA using a hierarchical approach and energetic evaluation with a continuum solvent model, *J. Mol. Biol. 289*, 261−275.
34. Fountain, M. A., Serra, M. J., Krugh, T. R., and Turner, D. H. (1996) Structural features of a six-nucleotide RNA hairpin loop found in ribosomal RNA, *Biochemistry 35*, 6539−6548.
35. Huang, S., Wang, Y., and Draper, D. (1996) Structure of a hexanucleotide RNA hairpin loop conserved in ribosomal RNAs, *J. Mol. Biol. 258*, 308−321.
36. Schweisguth, D., and Moore, P. (1997) On the conformation of the anticodon loops of initiator and elongator methionine tRNAs, *J. Mol. Biol. 267*, 505−519.
37. Sierzputowska-Gracz, H., Sochaka, E., Malkiewicz, A., Kuo, K., Gehrke, C. W., and Agris, P. F. (1987) Chemistry and structure of modified uridines in the anticodon, wobble position of transfer RNA are determined by thiolation, *J. Am. Chem. Soc. 109*, 7171−7177.
38. Phelps, S. S., Malkiewicz, A., Agris, P. F., and Joseph, S. (2004) Modified nucleotides in tRNA^{Lys} and tRNA^{Val} are important for translocation, *J. Mol. Biol. 338*, 439−444.
39. Neuhaus, D., and Williamson, M. (1989) *The Nuclear Overhauser Effect in Structural and Conformational Analysis*, VCH Publishers, New York.
40. Hatfield, D. L., and Gladyshev, V. M. (2002) How selenium has altered our understanding of the genetic code, *Mol. Cell. Biol. 22*, 3565−3576.
41. Jameson, R. R., and Diamond, A. M. (2004) A regulatory role for Sec tRNA$^{[Ser]Sec}$ in selenoprotein synthesis, *RNA 10*, 1142−1152.
42. Basti, M., Stuart, J., Lam, A., Guenther, R., and Agris, P. (1996) Design, biological activity, and NMR-solution structure of a DNA analogue of yeast tRNA^{Phe} anticodon domain, *Nat. Struct. Biol. 3*, 38−44.
43. Stuart, J. W., Gdaniec, Z., Guenther, R. H., Marszalek, M., Sochacka, E., Malkiewicz, A., and Agris, P. F. (2000) Functional anticodon architecture of human tRNA^{Lys,3} includes disruption of intraloop hydrogen bonding by the naturally occurring amino acid modification t^{6}A, *Biochemistry 39*, 13396−13404.
44. Murphy, F. V., Ramakrishnan, V., Malkiewicz, A., and Agris, P. F. (2004) The role of modifications in codon discrimination by tRNA$^{Lys}_{UUU}$, *Nat. Struct. Mol. Biol. 11*, 1186−1191.
45. Yusukawa, T., Suzuki, T., Ishii, N., Ohta, S., and Watanabe, K. (2001) Wobble modification defect in tRNA disturbs codon−anticodon interaction in a mitochondrial disease, *EMBO J. 20*, 4794−4802.
46. Reddy, P. R., Hamill, W. D., Chheda, G. B., and Schweizer, M. P. (1981) On the function of *N*-[(9-β-D-ribofuranosylpurin-6-yl)-carbamoyl] threonine in transfer ribonucleic acid. Metal ion binding studies, *Biochemistry 20*, 4979−4986.
47. Ogle, J. M., Broderson, D. E., Clemons, W. M., Tarry, M. J., Carter, A. P., and Ramakrishnan, V. (2001) Recognition of cognate transfer RNA by the 30S ribosomal subunit, *Science 292*, 897−902.

BI050343F